LAWRENCE
LIVERMORE
NATIONAL
LABORATORY

LLNL-JRNL-563431

A Block-Diagonal Algebraic Multigrid Preconditioner for the Brinkman Problem

P. S. Vassilevski, U. Villa

July 6, 2012

Siam Journal on Scientific Computing

Disclaimer

A BLOCK-DIAGONAL ALGEBRAIC MULTIGRID PRECONDITIONER FOR THE BRINKMAN PROBLEM *

PANAYOT S. VASSILEVSKI† AND UMBERTO VILLA ‡

Abstract. The Brinkman model is a unified law governing the flow of a viscous fluid in cavity (Stokes equations) and in porous media (Darcy equations). In this work, we explore a novel mixed formulation of the Brinkman problem by introducing the flow's vorticity as an additional unknown. This formulation allows for a uniformly stable and conforming discretization by standard finite element (Nédélec, Raviart-Thomas, discontinuous piecewise polynomials). Based on the stability analysis of the problem in the $H(\mathrm{curl}) - H(\mathrm{div}) - L^2$ norms ([24]), we study a scalable block diagonal preconditioner which is provably optimal in the constant coefficient case. Such preconditioner takes advantage of the parallel auxiliary space AMG solvers for $H(\mathrm{curl})$ and $H(\mathrm{div})$ problems available in hypre ([11]). The theoretical results are illustrated by numerical experiments.

Key words. Brinkman problem; Stokes-Darcy coupling; saddle-point problems; block preconditioners; algebraic multigrid.

Introduction. The Brinkman equations describe the flow of a viscous fluid in cavity and porous media. It was initially proposed in [1], [2] as a homogenization technique for the Navier-Stokes equations. Typical applications of this model are in underground water hydrology, petroleum industry, automotive industry, biomedical engineering, and heat pipes modeling.

Mathematically speaking the Brinkman model is a parameter-dependent combination of the Darcy and Stokes models. Since in real applications the number and the locations of the Stokes-Darcy interfaces might not be known *a priori*, the unified equations in the Brinkman model represent an advantage over the domain decomposition methods coupling the Darcy and the Stokes equations. However, the high variability in the PDE coefficients, that may take extremely large or small values, negatively affects the conditioning of the discrete problem which poses a substantial challenge for developing efficient preconditioners for this problem.

Another challenging aspect of the Brinkman model is the construction of a stable finite element discretization ([17], [25]). As a matter of fact, standard inf-sup compatible finite elements for both Stokes (Taylor Hood, P2-P0, Crouzeix-Raviart – P0, mini elements) or Darcy (Raviart-Thomas – P0 elements) lead to non-convergent discretizations: the first group suffers of stability issues in the limit Darcy case, whereas the second ones are not conforming in presence of viscosity. Numerous different approaches have been proposed in the literature to address the numerical stability of the discretization. Among those, penalization methods ([6], [7]), augmented Lagrangian and least squares stabilization approaches ([8]), or special high order non-conforming elements ([17], [9]) are some examples.

In the present paper, we consider the mixed formulation of the Brinkman problem proposed by the authors in [24]. Following what has already been done for the Stokes problem ([5], [3]), the authors introduced the (scaled) vorticity as additional unknown. The well-posedness analysis of the mixed formulation was based on the Hilbert complex structure for the Hodge Laplacian, and the numerical stability of the method

*This work was performed under the auspices of the U.S. Department of Energy by Lawrence Livermore National Laboratory under Contract DE-AC52-07NA27344.

† panayot@llnl.gov, Center for Applied Scientific Computing, Lawrence Livermore National Laboratory, P.O. Box 808, L-561, Livermore, CA 94551, U.S.A.

‡uvilla@emory.edu, Department of Mathematics and Computer Science, Emory University, Atlanta, GA 30322, U.S.A.

was guaranteed by an analogous result on the discrete level. The particular choice of Nédélec, Raviart-Thomas and piecewise discontinuous elements, in fact, reproduces the same embedding and mapping properties of the continuous spaces in the finite elements spaces. In contrast to the penalization methods for the Brinkman problem ([6], [7]), this approach allows for a conforming discretization by standard finite elements. Discretization errors in the $H(\mathrm{div})$-norm of the velocity and in the L^2-norm of the pressure exhibit uniform decay rates with respect to the inverse permeability coefficient $k(\mathbf{x})$. Only the (scaled) vorticity is approximated with less accuracy as the equations approach the Darcy limit ([24]).
A disadvantage of the mixed formulation approach is that the Hodge decomposition holds only for particular sets of boundary conditions ([3]).

In this work, we focus on the development of effective preconditioning techniques for the discrete saddle-point problem obtained after finite element discretization of the mixed formulation. Following the approach in [18], we construct a block diagonal preconditioner with optimal convergence properties based on the stability analysis of the continuous problem. Such preconditioner has on its main diagonal the finite element matrices corresponding to the $H(\mathrm{curl})$, $H(\mathrm{div})$, and L^2 norms involved in the stability estimates. To improve the efficiency of the preconditioner, we resort to the auxiliary space multigrid preconditioners for $H(\mathrm{div})$ and $H(\mathrm{curl})$ problems analyzed in [10] and further developed in [14], [15].

The remainder of the present paper is structured as follows. In Section 1, we briefly derive the mixed formulation of the Brinkman problem based on the Hodge Laplacian, and we provide a stability estimate. In Section 2, we address the numerical discretization of the mixed formulation with Nédélec, Raviart-Thomas and piecewise polynomial discontinuous finite element which leads to a large sparse saddle-point linear system. In Section 3, we derive an optimal preconditioner with respect to the mesh size. We also investigate an augmented Lagrangian approach in order to improve the robustness of the preconditioner with respect to the PDE coefficients. Finally, in Section 4 we present numerical results, including some parallel scalability tests, for the case of constant and space-dependent inverse permeability coefficient.

1. Mixed formulation of the Brinkman Problem. We assume that Ω is a bounded simply connected domain in $\mathbb{R}^d$ with a Lipschitz continuous simply connected boundary $\partial\Omega$ that has well-defined (almost everywhere) unit outward normal vector $\mathbf{n} \in \mathbb{R}^d$. The generalized Brinkman problem reads

$$\begin{cases} -\nu\, \Delta \mathbf{u} + k(\mathbf{x})\, \mathbf{u} + \nabla p = \mathbf{f}(\mathbf{x}), & \forall\, \mathbf{x} \in \Omega \\ \mathrm{div}\ \mathbf{u} = g(\mathbf{x}), & \forall\, \mathbf{x} \in \Omega \\ \mathbf{u} \times \mathbf{n} = \mathbf{g}, & \text{on } \partial\Omega \\ -p + \nu\, \mathrm{div}\ \mathbf{u} = h, & \text{on } \partial\Omega, \end{cases} \tag{1.1}$$

where $\nu \geq 0$ is the fluid viscosity and $k(\mathbf{x})$ is the inverse permeability of the medium. The challenge of this problems is when the coefficient $k = k(\mathbf{x})$ takes two extreme values $\mathcal{O}(1)$ and $\mathcal{O}(1/\epsilon)$ in different parts of Ω. In the part of the domain with $k = \mathcal{O}(1)$, the PDE behaves like a Stokes problem, whereas in the rest of the domain, it behaves like Darcy equations.

In the present work, for simplicity, we assume natural boundary conditions on $\partial\Omega$. However, other set of boundary conditions, like the essential boundary conditions ($\mathbf{u} \cdot \mathbf{n} = u_n$, $\boldsymbol{\sigma} \times \mathbf{n} = \boldsymbol{\sigma}_\tau$), can also be treated in a similar way. For the Hodge Laplacian, natural boundary conditions are also known in the literature as electric boundary conditions while the essential ones as magnetic boundary conditions due to

the close relation with Maxwell's equations. In our work, we do not consider the case of full Dirichlet boundary condition, as the mixed formulation is harder to analyze; it leads to suboptimal discretization error behavior ([3]).

To obtain a mixed formulation of the Brinkman problem (1.1), we exploit the vector calculus identity

$$\Delta \mathbf{u} = \nabla \text{ div } \mathbf{u} - \text{curl curl } \mathbf{u},$$

and we define the (scaled) vorticity variable

$$\boldsymbol{\sigma} = \varepsilon \text{ curl } \mathbf{u}, \ \varepsilon = \sqrt{\nu}.$$

After some straightforward manipulations, the mixed formulation reads

$$\begin{cases} \boldsymbol{\sigma} - \varepsilon \text{ curl } \mathbf{u} = 0, & \forall \, \mathbf{x} \in \Omega \\ \varepsilon \text{ curl } \boldsymbol{\sigma} - \varepsilon^2 \, \nabla(\text{div } \mathbf{u}) + k(\mathbf{x}) \, \mathbf{u} + \nabla p = \mathbf{f}(\mathbf{x}), & \forall \, \mathbf{x} \in \Omega \\ \text{div } \mathbf{u} = g(\mathbf{x}), & \forall \, \mathbf{x} \in \Omega \\ \mathbf{u} \times \mathbf{n} = \mathbf{g}, & \text{on } \partial\Omega \\ -p + \varepsilon^2 \text{ div } \mathbf{u} = h, & \text{on } \partial\Omega. \end{cases} \tag{1.2}$$

In what follows, we assume that the inverse permeability coefficient $k(\mathbf{x})$ belongs to $L^\infty(\Omega) \cap L^2(\Omega)$, and that the inverse permeability $k(\mathbf{x})$ and the viscosity ε^2 can not both vanish at the same time. Such assumptions imply that there exist constants $\kappa_{\min} > 0$ and $\kappa_{\max} < +\infty$, such that

$$0 < \kappa_{\min} \leq k(\mathbf{x}) + \varepsilon^2 \leq \kappa_{\max}. \tag{1.3}$$

1.1. Functional spaces and mixed variational formulation. We now introduce some notation used throughout the paper. In what follows, sometimes we borrow some terminology from the finite element exterior calculus, e.g. from [4, 5], without explicitly referring to these (or other) sources. However, we keep this to a minimum to ensure that the presentation is self-contained.
For vectorial functions $\mathbf{u}, \mathbf{v} \in \mathbf{L}^2(\Omega) = [L^2(\Omega)]^d$ and scalar functions $p, q \in L^2(\Omega)$, we write the inner products $(\mathbf{u}, \mathbf{v}) = \int_\Omega \mathbf{u} \cdot \mathbf{v} \, d\Omega$ and $(p, q) = \int_\Omega p \, q \, d\Omega$. Similarly, we denote by $\|\mathbf{v}\|$ and $\|p\|$ the norms induced by the respective inner products.
To come up with the weak formulation of the system (1.2), we introduce the functional spaces $\mathbf{Q}$, $\mathbf{R}$ and W, defined as

- $\mathbf{Q} \equiv H(\text{curl}, \Omega) := \left\{ \boldsymbol{\sigma} \in L^2(\Omega) | \text{ curl } \boldsymbol{\sigma} \in L^2(\Omega) \right\}$, equipped with the norm

$$\|\boldsymbol{\tau}\|^2_{\mathbf{Q}} = \|\boldsymbol{\tau}\|^2 + \|\text{curl } \boldsymbol{\tau}\|^2;$$

- $\mathbf{R} \equiv H(\text{div}, \Omega) := \left\{ \mathbf{u} \in L^2(\Omega) | \text{ div } \mathbf{u} \in L^2(\Omega) \right\}$, equipped with the norm

$$\|\mathbf{v}\|^2_{\mathbf{R}} = \|\mathbf{v}\|^2 + \|\text{div } \mathbf{v}\|^2;$$

- $W \equiv L^2(\Omega)$, equipped with the norm

$$\|q\|^2_W = \|q\|^2.$$

We denote with $\mathbf{Q}^*$, $\mathbf{R}^*$, and W^* the dual spaces of $\mathbf{Q}$, $\mathbf{R}$, and W, respectively. It is clear that in the case of essential (magnetic) boundary conditions, the respective

spaces $\mathbf{Q}$, $\mathbf{R}$ are proper subsets of $H(\mathrm{curl})$, $H(\mathrm{div})$; $\mathbf{Q}$, $\mathbf{R}$ then consist of functions with vanishing tangential or normal boundary traces.

The mixed variational formulation of the Brinkman problem (1.2), which is of our main interest, reads as follows.

PROBLEM 1.1. *Find* $(\boldsymbol{\sigma}, \mathbf{u}, p) \in \mathbf{Q} \times \mathbf{R} \times W$ *such that*

$$\left\{ \begin{array}{llll} m(\boldsymbol{\sigma},\boldsymbol{\tau}) & -c^*(\mathbf{u},\boldsymbol{\tau}) & = F(\boldsymbol{\tau}) & \forall\, \boldsymbol{\tau} \in \mathbf{Q} \\ -c(\boldsymbol{\sigma},\mathbf{v}) & -a(\mathbf{u},\mathbf{v}) - d(\mathbf{u},\mathbf{v}) \quad +b^*(p,\mathbf{v}) & = G(\mathbf{v}) & \forall\, \mathbf{v} \in \mathbf{R} \\ & b(\mathbf{u},q) & = H(q) & \forall\, q \in W \end{array} \right. \tag{1.4}$$

where

$$\begin{array}{ll} m(\boldsymbol{\sigma},\ \boldsymbol{\tau}) = (\boldsymbol{\sigma},\ \boldsymbol{\tau}), & \boldsymbol{\sigma},\ \boldsymbol{\tau} \in \mathbf{Q} \\ c(\boldsymbol{\sigma},\ \mathbf{v}) = \varepsilon\ (\mathrm{curl}\ \boldsymbol{\sigma},\ \mathbf{v}), & \boldsymbol{\sigma} \in \mathbf{Q},\ \mathbf{v} \in \mathbf{R}, \\ a(\mathbf{u},\ \mathbf{v}) = \varepsilon^2 (\mathrm{div}\ \mathbf{u},\ \mathrm{div}\ \mathbf{v}), & \mathbf{u},\ \mathbf{v} \in \mathbf{R}, \\ d(\mathbf{u},\mathbf{v}) = (k(\mathbf{x})\ \mathbf{u},\ \mathbf{v}), & \mathbf{u},\ \mathbf{v} \in \mathbf{R}, \\ b(\mathbf{u},q) = (\mathrm{div}\ \mathbf{u},\ q), & \mathbf{u} \in \mathbf{R},\ q \in W. \end{array} \tag{1.5}$$

$F \in \mathbf{Q}^*$, $G \in \mathbf{R}^*$, $H \in W^*$ are bounded functionals that take into account volume forces and boundary conditions.

The stability analysis of the mixed formulation was carried out by the authors in [24], following the analysis of the Hodge Laplacian in [5], [3]. Here, we summarize the main results.

Let $\varepsilon \geq 0$ and $k(\mathbf{x}) \in L^\infty(\Omega) \cap L^2(\Omega)$, $0 < \kappa_{\min} \leq k(\mathbf{x}) + \varepsilon^2 \leq \kappa_{\max}$ almost everywhere in Ω, and introduce the weighted norms in the spaces $\mathbf{Q}_w$, $\mathbf{R}_w$, W_w defined by

$$\|\boldsymbol{\tau}\|^2_{\mathbf{Q}_w} = \|\boldsymbol{\tau}\|^2 + \frac{\varepsilon^2}{\kappa_{\max}} \|\mathcal{C}\boldsymbol{\tau}\|^2, \quad \|\mathbf{v}\|^2_{\mathbf{R}_w} = \kappa_{\min} \|\mathbf{v}\|^2_{\mathbf{R}}, \quad \|q\|^2_{W_w} = \frac{1}{\kappa_{\max}} \|q\|^2. \tag{1.6}$$

THEOREM 1.1. *The bilinear form corresponding to the mixed problem, Problem 1.1,*

$$\begin{aligned} &B(\boldsymbol{\sigma}, \mathbf{u}, p; \boldsymbol{\tau}, \mathbf{v}, q) = \\ &\quad = m(\boldsymbol{\sigma},\boldsymbol{\tau}) - c^*(\mathbf{u},\boldsymbol{\tau}) - c(\boldsymbol{\sigma},\mathbf{v}) - a(\mathbf{u},\mathbf{v}) - d(\mathbf{u},\mathbf{v}) + b^*(p,\mathbf{v}) + b(\mathbf{u},q), \end{aligned} \tag{1.7}$$

is bounded and satisfies an inf-sup condition. More specifically, there exist two constants M and α depending only on the domain Ω such that

$$|B(\boldsymbol{\sigma}, \mathbf{u}, p; \boldsymbol{\tau}, \mathbf{v}, q)| \leq M \frac{\kappa_{\max}}{\kappa_{\min}} \|(\boldsymbol{\sigma}, \mathbf{u}, p)\|_{\mathbf{Q}_w \times \mathbf{R}_w \times W_w}\ \|(\boldsymbol{\tau}, \mathbf{v}, q)\|_{\mathbf{Q}_w \times \mathbf{R}_w \times W_w} \tag{1.8}$$

and

$$\inf_{(\boldsymbol{\tau},\mathbf{v},q) \in \mathbf{Q}\times\mathbf{R}\times W} \sup_{(\boldsymbol{\sigma},\mathbf{u},p) \in \mathbf{Q}\times\mathbf{R}\times W} \frac{B(\boldsymbol{\sigma}, \mathbf{u}, p; \boldsymbol{\tau}, \mathbf{v}, q)}{\|(\boldsymbol{\tau}, \mathbf{v}, q)\|_{\mathbf{Q}_w \times \mathbf{R}_w \times W_w}\ \|(\boldsymbol{\sigma}, \mathbf{u}, p)\|_{\mathbf{Q}_w \times \mathbf{R}_w \times W_w}} \geq \alpha. \tag{1.9}$$

The proof of the inf-sup condition is based on certain orthogonal decomposition of $\mathbf{Q}$ and $\mathbf{R}$ and respective Poincaré inequalities holding for one of the components in these orthogonal decompositions. We refer to [24] for the details.

As an immediate consequence of the above theorem, the following well–posedness result is obtained in [24].

THEOREM 1.2. *The generalized Brinkman problem, Problem 1.1, admits a unique solution and the following a priori estimate holds:*

$$\|\boldsymbol{\sigma}\|^2_{\mathbf{Q}_w} + \|\mathbf{u}\|^2_{\mathbf{R}_w} + \|p\|^2_{W_w} \leq C(\Omega)(\|F\|^2_{\mathbf{Q}^*_w} + \|G\|^2_{\mathbf{R}^*_w} + \|H\|^2_{W^*_w}).$$

Here $C(\Omega)$ is a constant depending only on the domain, and the weighted norms in the spaces $\mathbf{Q}_w$, $\mathbf{R}_w$, W_w are defined in (1.6).

2. Discretization. For a given integer $r \geq 0$, we let $\mathbf{Q}_h$ be the $(r+1)$-th order Nédélec finite elements ([20]), $\mathbf{R}_h$ the r-th order Raviart-Thomas finite elements ([23, 20]), and W_h the discontinuous piecewise polynomials finite element of degree at most r.

It is well-known ([19]) that the canonical interpolation operators $\Pi^{\mathbf{V}}_h : \mathbf{V} \mapsto \mathbf{V}_h$ ($\mathbf{V} := \mathbf{Q}$, $\mathbf{R}$, W) commute with the curl and div differential operators, that is

$$\text{curl}\, \Pi^{\mathbf{Q}}_h = \Pi^{\mathbf{R}}_h \text{curl}, \quad \text{and} \quad \text{div}\, \Pi^{\mathbf{R}}_h = \Pi^{W}_h \text{div}.$$

Indeed such spaces form a finite dimensional subcomplex of the continuous de Rham complex and give raise to the following commuting diagram ([4, 5]):

$$\begin{array}{ccccccc} H^1\backslash\mathbb{R} & \xrightarrow{\nabla} & \mathbf{Q} & \xrightarrow{\text{curl}} & \mathbf{R} & \xrightarrow{\text{div}} & W \\ \downarrow & & \downarrow & & \downarrow & & \downarrow \\ S_h\backslash\mathbb{R} & \xrightarrow{\nabla} & \mathbf{Q}_h & \xrightarrow{\text{curl}} & \mathbf{R}_h & \xrightarrow{\text{div}} & W_h \end{array} .$$

Here we also introduced the space S_h of continuous piecewise polynomial of degree at most $r+1$. Even though such space is not directly involved in the discretization of the Brinkman problem, it plays an important role in the construction of the auxiliary space multigrid preconditioner for $H(\text{curl})$ and $H(\text{div})$ problems ([10],[14, 15]).

Of our main interest is the Galerkin problem

PROBLEM 2.1. *Find $(\boldsymbol{\sigma}_h, \mathbf{u}_h, p_h) \in \mathbf{Q}_h \times \mathbf{R}_h \times W_h$ such that*

$$\left\{ \begin{array}{llll} m(\boldsymbol{\sigma}_h, \boldsymbol{\tau}_h) & -c^*(\mathbf{u}_h, \boldsymbol{\tau}_h) & & = F(\boldsymbol{\tau}_h) \quad \forall\, \boldsymbol{\tau}_h \in \mathbf{Q}_h \\ -c(\boldsymbol{\sigma}_h, \mathbf{v}_h) & -a(\mathbf{u}_h, \mathbf{v}_h) - d(\mathbf{u}_h, \mathbf{v}_h) & +b^*(p_h, \mathbf{v}_h) & = G(\mathbf{v}_h) \quad \forall\, \mathbf{v}_h \in \mathbf{R}_h \\ & b(\mathbf{u}_h, q_h) & & = H(q_h) \quad \forall\, q_h \in W_h \end{array} \right. \tag{2.1}$$

Since the discrete finite element spaces $\mathbf{Q}_h, \mathbf{R}_h, W_h$ preserve all the properties of the continuous spaces, the bilinear form B restricted to the discrete spaces satisfies the inf-sup condition (1.9) with a constant α_h bounded independently of h, and therefore the Galerkin problem is well-posed ([24]).

To come up with an algebraic form of Problem 2.1, we let $N_{\boldsymbol{\sigma}} = \dim(\mathbf{Q}_h)$, $N_{\mathbf{u}} = \dim(\mathbf{R}_h)$, $N_p = \dim(W_h)$ be the dimensions of the finite element spaces $\mathbf{Q}_h$, $\mathbf{R}_h$, W_h, and we introduce the vectors $\boldsymbol{\Sigma} \in \mathbb{R}^{N_{\boldsymbol{\sigma}}}$, $\mathbf{U} \in \mathbb{R}^{N_{\mathbf{u}}}$, $P \in \mathbb{R}^{N_p}$ collecting the finite element degrees of freedom $\boldsymbol{\sigma}^i_h$, $i = 1, \ldots, N_{\boldsymbol{\sigma}}$, $\mathbf{u}^i_h$, $i = 1, \ldots, N_{\mathbf{u}}$ and p^i_h, $i = 1, \ldots, N_p$. We also introduce the finite element matrices $M \in \mathbb{R}^{N_{\boldsymbol{\sigma}} \times N_{\boldsymbol{\sigma}}}$, $C \in \mathbb{R}^{N_{\mathbf{u}} \times N_{\boldsymbol{\sigma}}}$, $A \in \mathbb{R}^{N_{\mathbf{u}} \times N_{\mathbf{u}}}$, $D \in \mathbb{R}^{N_{\mathbf{u}} \times N_{\mathbf{u}}}$, $B \in \mathbb{R}^{N_p \times N_{\mathbf{u}}}$ whose entries are given by

$$\begin{array}{ll} M_{i,j} = m(\boldsymbol{\sigma}^j_h,\ \boldsymbol{\tau}^i_h) = (\boldsymbol{\sigma}^j_h,\ \boldsymbol{\tau}^i_h) & i,j = 1, \ldots, N_{\boldsymbol{\sigma}} \\ C_{i,j} = c(\boldsymbol{\sigma}^j_h,\ \mathbf{v}^i_h) = \varepsilon\ (\text{curl}\ \boldsymbol{\sigma}^j_h,\ \mathbf{v}^i_h) & i = 1, \ldots, N_{\mathbf{u}},\ j = 1, \ldots, N_{\boldsymbol{\sigma}} \\ A_{i,j} = a(\mathbf{u}^j_h,\ \mathbf{v}^i_h) = \varepsilon^2(\text{div}\ \mathbf{u}^j_h,\ \text{div}\ \mathbf{v}^i_h) & i,j = 1, \ldots, N_{\mathbf{u}} \\ D_{i,j} = d(\mathbf{u}^j_h,\ \mathbf{v}^i_h) = (k(\mathbf{x})\ \mathbf{u}^j_h,\ \mathbf{v}^i_h) & i,j = 1, \ldots, N_{\mathbf{u}} \\ B_{i,j} = b(\mathbf{u}^j_h,\ q^i_h) = (\text{div}\ \mathbf{u}^j_h,\ q^i_h) & i = 1, \ldots, N_p,\ j = 1, \ldots, N_{\mathbf{u}}. \end{array} \tag{2.2}$$

Letting $N = N_{\boldsymbol{\sigma}} + N_{\mathbf{u}} + N_p$ be the total number of unknowns, we write the linear system corresponding to the Brinkman problem as

$$\mathcal{B}\mathbf{X} = \mathbf{B} \tag{2.3}$$

where the block matrix $\mathcal{B} \in \mathbb{R}^{N\times N}$ and the block vectors $\mathbf{X} \in \mathbb{R}^N$ and $\mathbf{B} \in \mathbb{R}^N$ read

$$\mathcal{B} = \begin{bmatrix} M & -C^T & 0 \\ -C & -A-D & B^T \\ 0 & B & 0 \end{bmatrix}, \quad \mathbf{X} = \begin{bmatrix} \boldsymbol{\Sigma} \\ \mathbf{U} \\ P \end{bmatrix}, \quad \mathbf{B} = \begin{bmatrix} \mathbf{F} \\ \mathbf{G} \\ H \end{bmatrix}. \tag{2.4}$$

We also introduce the augmented formulation of the Brinkman problem that will be used in the numerical tests. Letting $M_W \in \mathbb{R}^{N_p\times N_p}$ be the pressure mass matrix and $\gamma \in \mathbb{R}$ a positive number, the augmented matrix and right-hand-side have the form

$$\mathcal{B}_\gamma = \begin{bmatrix} M & -C^T & 0 \\ -C & -A-D-\gamma B^T M_W^{-1} B & B^T \\ 0 & B & 0 \end{bmatrix}, \quad \mathbf{B}_\gamma = \begin{bmatrix} \mathbf{F} \\ \mathbf{G} - \gamma B M_W^{-1} H \\ H \end{bmatrix}. \tag{2.5}$$

The advantage of the augmented formulation is that it improves the inf-sup constant α, and therefore, it leads to the solution of better conditioned problems, provided that the augmentation parameter γ is not too large. In the numerical result presented in the following we take γ of the order of the inverse permeability coefficient k.

3. Preconditioning. The discretized linear system (2.3) has the form of a symmetric indefinite problem, having $N_{\boldsymbol{\sigma}} + N_p$ positive eigenvalues and $N_{\mathbf{u}}$ negative eigenvalues. An effective iterative method to solve linear system with symmetric indefinite matrices is MINRES ([21]) employing a symmetric positive definite preconditioner $\mathcal{P}$.

To derive the preconditioner, we follow the approach presented in ([18]) for preconditioning symmetric saddle-point problems in a functional space setting. According to the authors, the mapping properties of the differential operators of the continuous problem suggest that block diagonal preconditioners are natural choices for saddle-point problems. More specifically, given a stability estimate for the continuous problem in some functional spaces, the block diagonal matrix, in which the blocks represent the discretization of the inner products in those spaces, leads to a uniformly bounded (in terms of h) preconditioner for the saddle-point discrete system of interest.

Recalling the weights in (1.6), $w_Q = \frac{\varepsilon^2}{\kappa_{\max}}$, $w_R = \kappa_{\min}$, $w_W = \frac{1}{\kappa_{\max}}$, we introduce the symmetric positive definite variational forms

$$\begin{array}{lcll} q(\boldsymbol{\sigma}_h, \boldsymbol{\tau}_h) = & (\boldsymbol{\sigma}_h, \boldsymbol{\tau}_h) + w_Q(\operatorname{curl} \boldsymbol{\sigma}_h, \operatorname{curl} \boldsymbol{\tau}_h), & \boldsymbol{\sigma}_h, \boldsymbol{\tau}_h \in \mathbf{Q}_h \\ r(\mathbf{u}_h, \mathbf{v}_h) = & w_R(\mathbf{u}_h, \mathbf{v}_h) + w_R(\operatorname{div} \mathbf{u}_h, \operatorname{div} \mathbf{v}_h), & \mathbf{u}_h, \mathbf{v}_h \in \mathbf{R}_h \\ w(p_h, q_h) = & w_W(p_h, q_h), & p_h, q_h \in W_h. \end{array} \tag{3.1}$$

The above forms define weighted inner products in $\mathbf{Q}_w$, $\mathbf{R}_w$ and W_w.

Therefore (based on [18]), a uniform preconditioner for the saddle-point problem (2.3) is given by

$$\mathcal{P} = \begin{bmatrix} Q & 0 & 0 \\ 0 & R & 0 \\ 0 & 0 & W \end{bmatrix}, \tag{3.2}$$

where Q, R, W are the matrix representations of the weighted inner products $q(\boldsymbol{\sigma}_h, \boldsymbol{\tau}_h)$, $r(\mathbf{u}_h, \mathbf{v}_h)$, and $w(p_h, q_h)$.

We now proceed, for completeness, with the standard analysis of the spectral condition number $K(\mathcal{A})$ of the preconditioned saddle-point operator $\mathcal{A} = \mathcal{P}^{-\frac{1}{2}}\mathcal{B}\mathcal{P}^{-\frac{1}{2}}$. First of all, we remark that, if the vector $\hat{\mathbf{Y}} \in \mathbb{R}^N$ collects the degrees of freedom of the finite element functions $\boldsymbol{\tau}_h \in \mathbf{Q}_h$, $\mathbf{v}_h \in \mathbf{R}_h$, $q_h \in W_h$, then the $\mathcal{P}$ norm of $\hat{\mathbf{Y}}$ is equal to the norm of $(\boldsymbol{\tau}_h, \mathbf{v}_h, q_h)$ in $\mathbf{Q}_w \times \mathbf{R}_w \times W_w$, that is

$$\|\hat{\mathbf{Y}}\|_{\mathcal{P}} = \sqrt{\hat{\mathbf{Y}}^T\mathcal{P}\hat{\mathbf{Y}}} = \|(\boldsymbol{\tau}_h, \mathbf{v}_h, q_h)\|_{\mathbf{Q}_w \times \mathbf{R}_w \times W_w}.$$

Next, we recall the definition of the spectral condition number of an invertible (symmetric indefinite) operator $\mathcal{A}$,

$$K(\mathcal{A}) = \sup_{\mathbf{X}\in\mathbb{R}^N} \frac{\|\mathcal{A}\mathbf{X}\|_2}{\|\mathbf{X}\|_2} \sup_{\mathbf{Y}\in\mathbb{R}^N} \frac{\|\mathcal{A}^{-1}\mathbf{Y}\|_2}{\|\mathbf{Y}\|_2} = \frac{\max|\lambda|}{\min|\lambda|},\ \lambda \in \sigma(\mathcal{A}).$$

The aim now is to bound the two factors $\sup_{\mathbf{X}\in\mathbb{R}^N} \frac{\|\mathcal{A}\mathbf{X}\|_2}{\|\mathbf{X}\|_2}$ and $\sup_{\mathbf{Y}\in\mathbb{R}^N} \frac{\|\mathcal{A}^{-1}\mathbf{Y}\|_2}{\|\mathbf{Y}\|_2}$ by using the continuity and the inf-sup condition of the bilinear form B. For the first term, by letting $\hat{\mathbf{X}} = \mathcal{P}^{-\frac{1}{2}}\mathbf{X}$ and $\hat{\mathbf{Y}} = \mathcal{P}^{-\frac{1}{2}}\mathbf{Y}$ and by using (1.8), we have

$$\sup_{\mathbf{X}\in\mathbb{R}^N} \frac{\|\mathcal{A}\mathbf{X}\|_2}{\|\mathbf{X}\|_2} = \sup_{\mathbf{X}\in\mathbb{R}^N} \sup_{\mathbf{Y}\in\mathbb{R}^N} \frac{\mathbf{Y}^T\mathcal{A}\mathbf{X}}{\|\mathbf{Y}\|_2\,\|\mathbf{X}\|_2} = \sup_{\hat{\mathbf{X}}\in\mathbb{R}^N} \sup_{\hat{\mathbf{Y}}\in\mathbb{R}^N} \frac{\hat{\mathbf{Y}}^T\mathcal{B}\hat{\mathbf{X}}}{\|\hat{\mathbf{Y}}\|_{\mathcal{P}}\,\|\hat{\mathbf{X}}\|_{\mathcal{P}}} \le M\frac{\kappa_{\max}}{\kappa_{\min}}.$$

Similarly, by using the discrete version of the inf-sup condition (1.9), for the second term we have

$$\sup_{\mathbf{Y}\in\mathbb{R}^N} \frac{\|\mathcal{A}^{-1}\mathbf{Y}\|_2}{\|\mathbf{Y}\|_2} = \left(\inf_{\mathbf{X}\in\mathbb{R}^N} \frac{\|\mathcal{A}\mathbf{X}\|_2}{\|\mathbf{X}\|_2}\right)^{-1} = \left(\inf_{\mathbf{X}\in\mathbb{R}^N} \sup_{\mathbf{Y}\in\mathbb{R}^N} \frac{\mathbf{Y}^T\mathcal{A}\mathbf{X}}{\|\mathbf{Y}\|_2\,\|\mathbf{X}\|_2}\right)^{-1} =$$
$$\left(\inf_{\hat{\mathbf{X}}\in\mathbb{R}^N} \sup_{\hat{\mathbf{Y}}\in\mathbb{R}^N} \frac{\hat{\mathbf{Y}}^T\mathcal{B}\hat{\mathbf{X}}}{\|\hat{\mathbf{Y}}\|_{\mathcal{P}}\,\|\hat{\mathbf{X}}\|_{\mathcal{P}}}\right)^{-1} \le \frac{1}{\alpha_h}. \quad (3.3)$$

In conclusion, combining the last two inequalities above, we obtain the following result.

THEOREM 3.1. *The relative condition number of $\mathcal{B}$ with respect the block–diagonal preconditioner $\mathcal{P}$ satisfies the estimate*

$$K(\mathcal{P}^{-\frac{1}{2}}\mathcal{B}\mathcal{P}^{-\frac{1}{2}}) = \frac{\max|\lambda|}{\min|\lambda|} \le \frac{M}{\alpha_h}\frac{\kappa_{\max}}{\kappa_{\min}}.$$

The above estimate implies that in the particular case of constant inverse permeability $k(\mathbf{x}) = k_0$, the condition number of the preconditioned saddle-point problem is independent of both the mesh size and k_0. The numerical experiments in the following section confirm this claim. However, in the general case of variable coefficient $k(\mathbf{x})$, the condition number increases proportionally to the ratio $\frac{\kappa_{\max}}{\kappa_{\min}}$. To alleviate this issue, in the numerical results section, we introduce a special augmentation of the Brinkman problem and a modified version of the preconditioner, which gives optimal convergence rates for smooth coefficients $k(\mathbf{x})$.

Finally, we remark (as is well-known) that the operator $\mathcal{A} = \mathcal{P}^{-\frac{1}{2}}\mathcal{B}\mathcal{P}^{-\frac{1}{2}}$ above is introduced only for the purpose of the analysis, and it does not explicitly appear in the implementation of the preconditioned MINRES algorithm; indeed only applications of $\mathcal{P}^{-1}$ to a vector are required. Moreover, to make it practical, we substitute $\mathcal{P}^{-1}$ with a spectrally equivalent operator $\hat{P}^{-1}$ that is easier to apply (in fact, with optimal cost). In the numerical results section, we demonstrate that letting $\hat{P}^{-1}$ be an auxiliary space AMG preconditioner can drastically reduce the computational effort.

4. Numerical Results. The numerical results presented in the following aim to study the performance of the proposed preconditioner both in terms of number of iterations and wall time. Problems with increasing level of difficulty are considered: first the case when the inverse permeability coefficient $k(\mathbf{x})$ is constant in the domain, then when it varies smoothly, and finally we illustrate the difficulties with the block–diagonal preconditioning approach when the coefficient $k(\mathbf{x})$ admits large jumps.

Concerning the choice of the finite element spaces, we will restrict ourselves to the case $r = 0$, i.e. first order Nédélec elements, lowest order Raviart-Thomas elements, and piecewise constant elements. This is not a limitation of the method since, in many practical applications, only discretization error of first order can be achieved due to non-smooth exact solutions and to discontinuities in the PDE coefficients.

Two different versions of the block-diagonal preconditioner in (3.2) are compared. In the exact (*ideal*) version the blocks Q, R are solved exactly by using the preconditioned conjugate gradient method; while in the AMG (*practical*) version the inverse of blocks Q, R are approximated by one V-cycle for the auxiliary space AMG for $H(\text{curl})$ and $H(\text{div})$ problem respectively.

In practice the AMG version of the preconditioner out-performs the exact one, but we remark the theoretical importance of the latter, since it allows us to confirm the theoretical, uniform with respect to the mesh, performance of the preconditioner.

In both versions of the preconditioner, the block W is inverted exactly. Indeed, due to the choice of discontinuous pressure finite elements W has a block diagonal structure, and it reduces to a diagonal matrix for piecewise constant elements.

Before discussing in detail the obtained numerical results, we describe briefly the software, compilers and hardware that we have used.

Concerning the finite element discretization of the Brinkman problem, we used the parallel C++ library MFEM [http://code.google.com/p/mfem/], developed at Lawrence Livermore National Laboratory (LLNL). This library supports a wide variety of finite element spaces in 2D and 3D, as well as many bilinear and linear forms defined on them. It includes classes for dealing with various types of triangular, quadrilateral, tetrahedral and hexahedral meshes and their global and local refinement. Parallelization in MFEM is based on MPI, and it leads to high scalability in the finite element assembly procedure. It supports several solvers from the hypre library (http://www.llnl.gov/CASC/hypre/). In particular, in our tests we used the auxiliary space algebraic multigrid solvers for $H(\text{curl})$ and $H(\text{div})$ ([14], [15]).

The initial meshes used in our simulation were generated with the unstructured mesh generator *Netgen* [http://www.hpfem.jku.at/netgen/].

The numerical results presented in this section were obtained on *hera*, a high performance computer at LLNL. *Hera* has a total of 864 nodes connected by InfiniBand DDR (Mellanox). Each node has 16 AMD Quad-Core Opteron 2.3Ghz CPUs, and 32GB of memory. *Hera* is running CHAOS 4.4, a Linux kernel developed at LLNL, specific for high performance computing.

Our code was compiled with the Intel *mpiicc* and *mpiicpc* compilers version 11.1.046.

4.1. Constant coefficient weak scalability test. We study the performance of the proposed preconditioner in the case of constant coefficient $k(\mathbf{x}) = k_0$. In particular, we present results relative to the augmented formulation (2.5) with $\gamma = k_0$ and the block diagonal preconditioner $\mathcal{P}$, where the weights w_Q, w_R, w_W are given

by

$$w_Q = \frac{\varepsilon^2}{k_0 + \varepsilon^2}, \quad w_R = k_0 + \varepsilon^2, \quad w_W = \frac{1}{k_0 + \varepsilon^2}. \tag{4.1}$$

For this test we use three different meshes in which the number of elements doubles from the previous to the next. By alternating between the three meshes and by using uniform refinements on each of them, we are able to build a sequence of discrete Brinkman problems whose size doubles each time. The sizes of the three meshes at the coarser level of refinement are given in Table 4.1. We use Metis ([13]) for the partitioning of the mesh among the processors.

Throughout the simulations we choose the number of processes in order to keep the number of unknowns per processor as constant as possible as we increase the total number of unknowns. We equally distribute the number of processes on each node of the parallel machine and we try to balance concurrency inside the node, on the one hand, with communications between nodes, on the other. In particular, we always use maximum a quarter of the total node capacity, in order to minimize overhead due to concurrent access to memory. In particular, we start with only one node and we run 1, 2, and 4 parallel processes, then we move to 8 nodes and we run 8, 16, 64 parallel processes (i.e. 1, 2, 4 processes per node, respectively), and so on.

In Table 4.2 we verify the uniform, with respect to the mesh, performance of the exact version of the preconditioner. The outer tolerance of MINRES is set to 10^{-10} while the inner tolerance of the PCG (for inverting the blocks of $\mathcal{P}$) is set to 10^{-12}. The number of iterations is uniformly bounded for every value of k. Beside the case $k = 10^6$ in which, we observe a moderate increase of the iteration numbers (while decreasing h), the preconditioner shows a perfectly uniform behavior.

In Table 4.3, we show the number of iterations when using a single V-cycle of the auxiliary space AMG preconditioners for $H(\mathrm{curl})$ and $H(\mathrm{div})$, keeping all other parameters in the test the same as before. For fixed k, we observe a moderate increase of the number of iterations as the number of unknowns is growing. This is expected, given the particular choice of the parameters in the V-cycle which are made in order to minimize wall time instead of number iterations. We refer to [14] for a more detailed discussion about the choice of the multigrid parameters and their effects on number of iterations for the auxiliary space AMG preconditioner for $H(\mathrm{curl})$ problems. Regarding the dependency of the iteration count with respect to the value of k, we notice that in the AMG version the number of iterations (even somewhat higher) is quite homogeneous with respect to k (for fixed mesh size).

Finally, in Table 4.4, we report the wall time to set-up the preconditioner (t_{setup}) and to solve iteratively the linear system with MINRES (t_{solve}). Timings are computed by using the *mpi* function `MPI_Wtime()`. The computation of the preconditioner consists in two phases. First we assemble the finite element matrices for the variational forms $q(\boldsymbol{\sigma}_h, \boldsymbol{\tau}_h)$, $r(\mathbf{u}_h, \mathbf{v}_h)$, and $w(p_h, q_h)$. Then, we compute the parameters (interpolation and coarse-level matrices) needed to build the auxiliary space solvers and to apply the V-cycle. We show only one column for t_{setup} since the preconditioner set-up is independent of the values of k. t_{setup} is usually negligible compared to t_{solve} (less than 10% in all cases), and it scales well (even if not perfectly) with the number of processes. The fact that for $np = 16$ and $np = 128$ it is faster than in the cases $np = 8$ and $np = 64$, respectively, may suggest some load unbalance due to the partition of the meshes in the latter case. With respect to the solution times t_{solve}, we notice that for a fixed problem size they tend to decrease as we approach the Darcy

	n_t	n_f	n_e
mesh 1	30336	62336	37940
mesh 2	57472	118304	72164
mesh 3	129920	266448	161602

TABLE 4.1

Number of elements n_t, faces n_f, and edges n_e on the coarser level of each unstructured mesh.

N	Number of MINRES iterations (Exact Preconditioner)						
	$k=0$	$k=10^{-6}$	$k=10^{-3}$	$k=1$	$k=10^{3}$	$k=10^{6}$	$\nu=0$
130612	16	16	16	18	30	17	10
247940	16	16	16	18	30	18	10
557970	16	16	16	18	30	20	10
1027944	16	16	16	18	30	20	10
1949480	16	16	16	18	30	22	10
4396980	16	16	16	18	30	23	10
8156368	16	16	16	18	30	23	10
15460560	16	16	16	18	30	25	10
34910120	16	16	16	18	30	27	10

TABLE 4.2

Number of MINRES iterations with the exact preconditioner for different values of k. N represents the total number of unknowns.

limit since less iterations are required to converge. For fixed k the scaling of t_{solve} with respect to the number of processors is similar to the one reported in [14] up to 128 processes, but we observe a severe loss of scalability when we use 256 processes. Possible causes of this loss of performance could be not perfect load balancing and hardware configuration issues, which are beyond the scope of this work.

4.2. The case of non-constant smooth coefficients. Now we consider the case of non-constant coefficient $k(\mathbf{x})$. For $\Omega = [0,1]^3$ and $c \leq 1$ being a positive number, we take

$$k(\mathbf{x}) = \frac{1}{\sin(\pi y)\sin(\pi z) + c} \quad \forall\, \mathbf{x} = (x, y, z) \in \Omega. \tag{4.2}$$

The number c controls how large are the variations in the coefficient $k(\mathbf{x})$, since $k(\mathbf{x})$ ranges between $k_{\min} \sim 1$ and $k_{\max} \sim \frac{1}{c}$. We let the viscosity be $\nu = \varepsilon^2 = 1$ and we choose the right hand side and the natural boundary conditions on $\partial\Omega$ be such that the analytical solution is given by

$$\boldsymbol{\sigma}_{exact} = \begin{bmatrix} 0 \\ \pi \sin(\pi y)\cos(\pi z) \\ -\pi \cos(\pi y)\sin(\pi x) \end{bmatrix}, \qquad \mathbf{u}_{exact} = \begin{bmatrix} \sin(\pi y)\sin(\pi z) \\ 0 \\ 0 \end{bmatrix}, \qquad p_{exact} = -x.$$

The computational domain Ω is discretized with an initial unstructured tetrahedral mesh with 474 elements. The original mesh is then uniformly refined 5 times, where each element of the mesh is divided in 8 ones using bisection. The total number of degrees of freedom ranges from around 2 thousand unknowns on the coarsest mesh up to 65 million on the finest mesh.

For this test, we extend the augmentation technique discussed before to the case of

	Number of MINRES iterations (AMG Preconditioner)						
N	$k=0$	$k=10^{-6}$	$k=10^{-3}$	$k=1$	$k=10^{3}$	$k=10^{6}$	$\nu=0$
130612	44	44	44	36	37	32	21
247940	48	48	48	40	39	34	23
557970	51	51	51	46	43	37	24
1027944	57	57	57	48	49	39	26
1949480	60	60	60	51	50	40	27
4396980	61	61	61	52	52	42	28
8156368	68	69	68	61	55	43	28
15460560	72	73	72	64	58	44	30
34910120	72	72	72	65	59	45	30

TABLE 4.3

Number of MINRES iterations with the AMG preconditioner for different values of k. N represents the total number of unknowns.

			t_{solve} (AMG Preconditioner)							t_{setup}
nn	np	N	$k=0$	$k=10^{-6}$	$k=10^{-3}$	$k=1$	$k=10^{3}$	$k=10^{6}$	$\nu=0$	
1	1	130612	15.2	15.1	15.1	12.7	13.0	11.3	8.0	0.71
1	2	247940	17.7	17.7	17.7	15.1	14.7	13.0	9.5	0.96
1	4	557970	22.6	22.5	22.5	19.5	19.4	16.8	11.9	1.28
8	8	1027944	25.6	25.2	24.9	21.6	21.9	17.5	13.0	1.47
8	16	1949480	26.8	26.9	26.8	22.8	22.6	18.4	13.7	1.42
8	32	4396980	33.0	33.0	33.1	28.3	28.6	22.9	17.0	1.74
64	64	8156368	36.2	36.8	36.7	33.2	30.6	24.5	20.1	2.15
64	128	15460560	45.3	44.8	44.9	41.5	35.7	28.3	22.0	1.76
64	256	34910120	90.0	91.7	91.0	83.2	76.7	52.3	43.6	2.56

TABLE 4.4

Computational cost of the AMG preconditioner. nn is the number of nodes used, np is the number of processes, N the total number of degrees of freedom, t_{solve} and t_{setup} measures the time in seconds to solve the linear system and to assemble the preconditioner, respectively.

non constant coefficient. In particular, we solve the augmented saddle-point problem

$$\begin{cases} (\boldsymbol{\sigma}_h, \boldsymbol{\tau}_h) - \varepsilon\,(\mathbf{u}_h, \operatorname{curl} \boldsymbol{\tau}_h) = F(\boldsymbol{\tau}_h), \quad \forall\, \boldsymbol{\tau}_h \in \mathbf{Q}_h \\ -\varepsilon\,(\operatorname{curl} \boldsymbol{\sigma}_h, \mathbf{v}_h) - (k(\mathbf{x})\,\mathbf{u}_h, \mathbf{v}_h) - ((k(\mathbf{x})+\varepsilon^2)\operatorname{div} \mathbf{u}_h, \operatorname{div} \mathbf{v}_h) + (p_h, \operatorname{div} \mathbf{u}_h) = \\ \qquad\qquad G(\mathbf{v}_h) + H(k(\mathbf{x})\operatorname{div} \mathbf{v}_h), \quad \forall\, \mathbf{v}_h \in \mathbf{R}_h \\ (\operatorname{div} \mathbf{u}_h, q_h) = H(q_h), \quad \forall\, q_h \in W_h \end{cases} \tag{4.3}$$

preconditioned by a block-diagonal preconditioner with blocks corresponding to the following bilinear forms:

$$\begin{cases} (\boldsymbol{\sigma}_h,\ \boldsymbol{\tau}_h) + \varepsilon^2 \left(\dfrac{1}{k(\mathbf{x})+\varepsilon^2} \operatorname{curl} \boldsymbol{\sigma}_h,\ \operatorname{curl} \boldsymbol{\tau}_h \right) & \boldsymbol{\sigma}_h, \boldsymbol{\tau}_h \in \mathbf{Q}_h \\ \big((k(\mathbf{x})+\varepsilon^2)\,\mathbf{u}_h,\ \mathbf{v}_h\big) + \big((k(\mathbf{x})+\varepsilon^2)\operatorname{div} \mathbf{u}_h,\ \operatorname{div} \mathbf{v}_h\big) & \mathbf{u}_h, \mathbf{v}_h \in \mathbf{R}_h \\ \left(\dfrac{1}{k(\mathbf{x})+\varepsilon^2}\, p_h,\ q_h \right) & p_h, q_h \in W_h. \end{cases} \tag{4.4}$$

In Table 4.5, we report the number of MINRES iterations for the solutions of the Brinkman problem with variable coefficients (stopping criterion: norm of the relative residual less or equal to 10^{-10}). We show both the exact and inexact block-diagonal preconditioner. The exact preconditioner shows perfect uniformity with

	Exact n_{it}			AMG n_{it}		
N	$\frac{k_{\max}}{k_{\min}} = 2$	$\frac{k_{\max}}{k_{\min}} \approx 10^3$	$\frac{k_{\max}}{k_{\min}} \approx 10^6$	$\frac{k_{\max}}{k_{\min}} = 2$	$\frac{k_{\max}}{k_{\min}} \approx 10^3$	$\frac{k_{\max}}{k_{\min}} \approx 10^6$
2.24K	19	30	30	26	35	36
16.9K	19	29	30	32	37	38
130K	19	29	32	46	45	48
1.03M	19	27	32	52	49	53
8.16M	19	27	32	63	61	61
65M	19	27	32	74	70	70

TABLE 4.5

Performances of the exact and AMG preconditioner for variable coefficient problem as a function of the ratio $\frac{k_{\max}}{k_{\min}}$. N represents the total number of unknowns and n_{it} the number of preconditioned MINRES iterations to achieve a relative reduction of the residual norm up to 10^{-10}.

respect to the mesh behavior, and a moderate dependence on the ratio $\frac{k_{\max}}{k_{\min}}$. The inexact preconditioner consists of one V-cycle of the auxiliary space AMG applied to the weighted $H(\text{curl})$ and $H(\text{div})$ variational forms in (4.4). The number of iterations tends to grow as we refine the mesh, but it is more uniform respect to the ratio $\frac{k_{\max}}{k_{\min}}$.

4.3. The case of coefficients with discontinuities. For this test, we consider the analytical solution of the so-called *circular preferential flow pathway* proposed in [12]. Such solution describes the steady flow of an incompressible fluid through a circular channel of radius R and length L in an infinite porous medium in response to a constant pressure gradient $\frac{\Delta p}{L}$ in the direction of the channel. Inside the preferential channel the inverse permeability is 0 (Stokes equations), outside is constant and equal to k. In Figure 4.1, we show the velocity and vorticity profiles in the radial direction. The velocity is continuous and differentiable with respect to the distance r from the center of the channel for each value of k, while the vorticity has a jump in the radial derivative at the interface between the preferential channel and the porous media ($r = R$). Moreover for large value of k, we observe a boundary layer in the porous media next to the interface with the preferential channel. In Figure 4.2, we show the three-dimensional solution computed on the finest mesh.

The geometry for this test is a cylinder of radius 2 and length $L = 1$. Inside this cylinder we embed a cylinder of radius $R = 1$ representing the preferential channel. The total number of degrees of freedom ranges from three thousand on the coarser level to 10 million on the finest.

In Table 4.6, we report the number of MINRES iteration required to achieve a reduction of 10^{-10} in the relative residual norm. Both, for the exact and AMG version of the preconditioner, the number of iterations highly depends on the size of the jump in the inverse permeability coefficient. In particular, for inverse permeability of the porous media up to 100, the qualitatively behavior of the preconditioner is the same as the constant and smoothly variable coefficient case: the number of iterations is uniform with respect to the mesh for the exact version, whereas for the AMG version it moderately increases as the mesh is refined. On the contrary, for higher values of the inverse permeability, the number of iterations tends to double at each mesh refinement for both versions of the preconditioner. Indeed, efficient preconditioning of the linear system with large jumps in the coefficient requires the introduction of a specialized coarse space correction and it is a subject of further investigation.

Conclusions. In this paper, we constructed an efficient and scalable preconditioner for the mixed formulation of the Brinkman problem proposed by the authors in

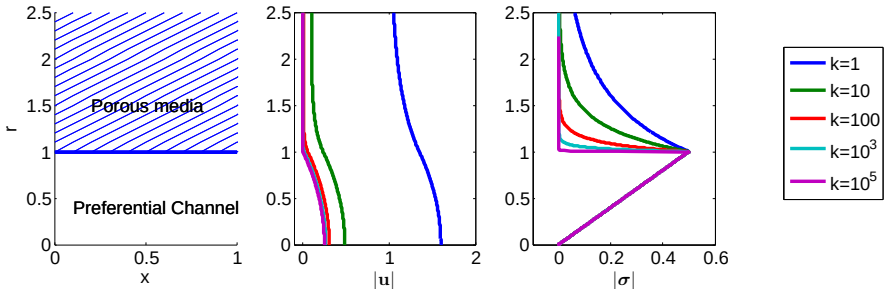

FIG. 4.1. *Velocity and vorticity profiles in the radial direction for different values of k.*

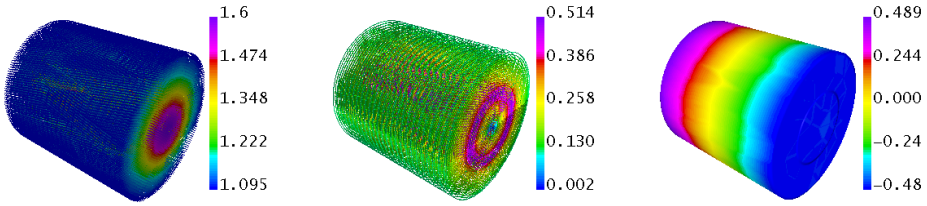

FIG. 4.2. *Numerical solution of the preferential channel on the finest grid ($k = 1$): velocity on the left, vorticity in the center, pressure on the right.*

[24]. The algebraic saddle-point system obtained after finite elements discretization can be efficiently solved with Krylov iterative methods using block diagonal AMG preconditioners. In particular, we used the auxiliary space algebraic multigrid preconditioners for $H(\text{curl})$ and $H(\text{div})$ for the vorticity and velocity block respectively, and diagonal scaling for the pressure block. In the case of constant and smooth PDE coefficients, the proposed preconditioner exhibits fairly scalable properties and it is robust with respect to a wide range of values of the inverse permeability coefficient $k(\mathbf{x})$.

Future developments of interest include upscaling techniques and construction of coarse hierarchies that respects the de Rham complex with good approximation properties to handle the non-constant coefficient case with both upscaling and solver (multigrid) purpose. For some progress in that direction, exploiting element-based algebraic multigrid (AMGe), we refer to [22] and [16].

REFERENCES

[1] G. ALLAIRE, *Homogenization of the Navier-Stokes equations in open sets perforated with tiny holes I. Abstract framework, a volume distribution of holes*, Archive for Rational Mechanics and Analysis, 113 (1991), pp. 209–259. 10.1007/BF00375065.

[2] ———, *Homogenization of the Navier-Stokes equations in open sets perforated with tiny holes II: Non-critical sizes of the holes for a volume distribution and a surface distribution of holes*, Archive for Rational Mechanics and Analysis, 113 (1991), pp. 261–298. 10.1007/BF00375066.

[3] D. N. ARNOLD, R. S. FALK, AND J. GOPALAKRISHNAN, *Mixed finite element approximation of the vector Laplacian with Dirichlet boundary conditions*. arXiv 1109.3668, submitted to Mathematical Models & Methods in Applied Sciences, 2011.

[4] D. N. ARNOLD, R. S. FALK, AND R. WINTHER, *Finite element exterior calculus, homological*

	Exact preconditioner n_{it}				
N	$k=1$	$k=10$	$k=10^2$	$k=10^3$	$k=10^5$
2.9K	28	40	92	129	121
21K	27	38	94	189	221
164K	25	36	90	202	393
1.3M	23	34	83	199	640
10M	23	31	79	186	868

	AMG preconditioner n_{it}				
N	$k=1$	$k=10$	$k=10^2$	$k=10^3$	$k=10^5$
2.9K	30	43	93	133	135
21K	30	43	100	199	271
164K	31	44	105	235	526
1.3M	34	48	112	264	921
10M	40	57	128	293	> 999

TABLE 4.6

Number of MINRES iterations to achieve a reduction of 10^{-10} *for the relative residual norm in the preferential channel test case.*

techniques, and applications, Acta Numerica, 15 (2006), pp. 1–155.

[5] ———, *Finite element exterior calculus: from Hodge theory to numerical stability*, Bull. Amer. Math. Soc. (N.S.), 47 (2010), pp. 281–354. DOI: 10.1090/S0273-0979-10-01278-4.

[6] E. Burman and P. Hansbo, *Stabilized Crouzeix-Raviart element for the Darcy-Stokes problem*, Numerical Methods for Partial Differential Equations, 21 (2005), pp. 986–997.

[7] ———, *A unified stabilized method for Stokes' and Darcy's equations*, Journal of Computational and Applied Mathematics, 198 (2007), pp. 35 – 51.

[8] M. R. Correa and A. F. D. Loula, *A unified mixed formulation naturally coupling Stokes and Darcy flows*, Computer Methods in Applied Mechanics and Engineering, 198 (2009), pp. 2710 – 2722.

[9] J. Guzmán and M. Neilan, *A family of nonconforming elements for the Brinkman problem*, IMA Journal of Numerical Analysis, (2012).

[10] R. Hiptmair and J. Xu, *Nodal auxiliary space preconditioning in H(curl) and H(div) spaces*, SIAM Journal on Numerical Analysis, 45 (2007), pp. 2483–2509.

[11] hypre *: High performance preconditioners*. http://www.llnl.gov/CASC/hypre/.

[12] A. A. Jennings and R. Pisipati, *The impact of Brinkman's extension of Darcy's law in the neighborhood of a circular preferential flow pathway*, Environmental Modelling and Software with Environment Data News, 14 (1999), pp. 427–435.

[13] G. Karypis and V. Kumar, *MeTis: Unstructured Graph Partitioning and Sparse Matrix Ordering System, Version 4.0*. http://www.cs.umn.edu/ metis, 2009.

[14] T. Kolev and P. S. Vassilevski, *Parallel Auxiliary Space AMG for H(curl) Problems*, J. of Computational Mathematics, 27 (2009).

[15] ———, *Parallel Auxiliary Space AMG Solver for H(div) Problems*. Technical Report LLNL-JRNL-520391, December 15, 2011.

[16] I. V. Lashuk and P. S. Vassilevski, *Element Agglomeration Coarse Raviart-Thomas Spaces With Improved Approximation Properties*, Numerical Linear Algebra with Applications, 19 (2012), pp. 414–426.

[17] K. A. Mardal, X. C. Tai, and R. Winther, *A Robust Finite Element Method for Darcy–Stokes Flow*, SIAM J. Numer. Anal., 40 (2002), pp. 1605–1631.

[18] K. A. Mardal and R. Winther, *Preconditioning discretizations of systems of partial differential equations*, Numerical Linear Algebra with Applications, 18 (2011), pp. 1–40.

[19] P. Monk, *Finite Element Methods for Maxwell's Equations*, Numerical Mathematics and Scientific Computation, Oxford University Press, Oxford, UK, 2003.

[20] J. C. Nédélec, *Mixed finite elements in* R^3, Numerische Mathematik, 35 (1980), pp. 315–341. 10.1007/BF01396415.

[21] C. C. Paige and M. A. Saunders, *Solution of sparse indefinite systems of linear equations*, SIAM J. Numerical Analysis, (1975), pp. 617–629.

[22] J. E. Pasciak and P. S. Vassilevski, *Exact de Rham Sequences of Spaces Defined on Macro-*

elements in Two and Three Spatial Dimensions, SIAM J. on Scientific Computing, 30 (2008), pp. 2427–2446.

[23] P. A. Raviart and J. M. Thomas, *A mixed finite element method for 2nd order elliptic problems*, Mathematical Aspects of the Finite Element Method, Lecture Notes in Mathematics, 606 (1977), pp. 292–315.

[24] P. S. Vassilevski and U. Villa, *A mixed formulation for the Brinkman problem*. in preparation, 2012.

[25] X. P. Xie, J. C. Xu, and G. R Xue, *Uniformly-stable finite element methods for Darcy-Stokes-Brinkman models* , J. Comput. Math., (2008).